# Behavior of a Round Cryogenic Jet at Below and Above the Critical Pressure

*B. Chehroudi*[*], *D. Talley*[#], *and E. Coy* [@]
Air Force Research Laboratory, 10 E. Saturn Boulevard, Edwards AFB, CA 93524-7680
Tel: (805) 275-6175, Fax: (805) 275-6245
The Tenth Annual Propulsion Symposium, Propulsion Engineering Research Center (PERC) at Penn State
NASA Marshall Space Flight Center, Hunstville, Alabama, October 26-27, 1998
*Raytheon STX, #Air Force Research Laboratory, @Air Force Research Laboratory

## ABSTRACT

In an effort to investigate and understand the behavior of the injected cryogenic fluid and its environment, a high pressure chamber is used into which pure $N_2$, He, and $O_2$ fluids are injected. Several chamber media are selected including, $N_2$, He, and mixtures of $CO+N_2$. The effects of chamber pressure ranging from a subcritical to a supercritical values at a supercritical chamber are photographically observed and documented near the injector hole exit region using a CCD camera illuminated by a short-duration back-lit strobe light. At low subcritical chamber pressures, the jets exhibit small surface irregularities that amplify downstream, looking intact, shiny, but wavy on the surface which eventually break up into irregularly-shaped small entities. Further increase of chamber pressure aids formation of many small droplets on the surface of the jet ejecting away only within a narrow region below the critical pressure of the injected fluid similar to a second wind-induced jet breakup regime. Raising the chamber pressure, transition into a full atomization regime is inhibited by reaching near, but slightly lower than, the critical pressure of the injectant where both surface tension and heat of vaporization are sufficiently reduced. The jet appearance changes abruptly at this point and remains the same to resemble a turbulent gas jet injection. The jet initial growth rate, is extracted from a large set of images and plotted with the available data on liquid fuel injection in diesel engine environment, turbulent incompressible, and variable density jets and mixing layers, creating a unique plot on its own. The jet spreading rate measurements agree well with a theoretical equation proposed for incompressible but variable density turbulent mixing layers by *Papamoschou and Roshko [1]* and follow the trend of that of *Dimotakis's [2]*, thus quantitatively strengthening the gas-jet like appearance. Considering this agreement, the inhibition of transition to atomization regime, and the visual nonexistence of drops; the relevancy of current injection models and some drop vaporization/combustion results under conditions where gas-jet like appearance is observed should be reexamined.



## INTRODUCTION

In designs of chemical rocket engines liquid fuel and oxidizer are injected through holes forming round jets, coaxial or impinging types, entering into the hot and elevated pressure environment of the combustion chamber. Progressively higher thrust chamber pressures are employed to achieve higher specific impulse and because of this trend and existence of high temperature in the combustor, injected liquid may find itself near or even above the thermodynamic critical condition. For example, the combustion chamber pressure for Vulcain (Ariane 5) with liquid $H_2$/liquid $O_2$ can reach up to 10 MPa while a record pressure of nearly 28.2 MPa has been reported by others. Very little information is available on liquid jets injected into supercritical condition. And this leads to our motivation in initiating an organized and systematic experimental effort investigating liquid jets under sub- and supercritical conditions.

There are drastic changes in some important properties of a pure substance as it approaches the thermodynamic critical point (CP). For example, under thermodynamic equilibrium condition, the distinction between liquid and gas phases disappears at and above the critical point and it is simply referred to as "fluid. Also, large changes of density occurs near the critical point. Other properties that change widely near the critical point are thermal conductivity, mass diffusivity, and surface tension. Indeed, constant-pressure specific heat becomes very large and surface tension vanishes at the critical point. Also, as ambient pressure is raised the importance of the

solubility of gases into the liquid phase increases and one should consider multicomponent phase equilibrium information. For example, for a pure hydrocarbon drop in a nitrogen environment, the amount of nitrogen dissolved on the surface of the liquid drop increases with pressure and, in addition, critical mixing temperature declines, see *Lazar and Faeth [3]*. In what follows, unless otherwise made clear, the terms sub- and supercritical and relative pressure and temperature are referenced with respect to the critical condition of the pure substance used in jets and not the environment.

There are a few works on liquid injection into supercritical condition, notably *Newman and Brzustowski [4]* and *Mayer et al.[5], [6]. Newman and Brzustowski [6]* use steady $CO_2$ jet injected into a chamber of pure $N_2$ and mixtures of $N_2$+$CO_2$ at both sub- and supercritical pressures and temperatures. In experiments where $CO_2$ is injected into a mixture of $CO_2$+$N_2$ with constant but large initial $CO_2$ mass fraction at a fixed supercritical temperature but varying sub- to supercritical pressures, they conjecture possibility of gasification and that at supercritical temperatures and pressures the jet may be considered as a variable-density single-phase turbulent submerged gas jet. *Mayer et al [6]* use liquid $N_2$ ($LN_2$) jet at 105 K into a $N_2$ environment at 300 K but at varying ambient pressures ranging from sub- to supercritical conditions and observe drastic changes in the jet structure near and above the critical pressure. The jet behaves similar to the classical atomization of liquid fuel with ligaments and drops near the critical pressure. They attribute this behavior to a continual decline of surface tension until it vanishes at and beyond critical point. They report no evidence of droplets at supercritical combustion.

## EXPERIMENTAL SETUP

Figure 1 shows schematic drawing of the experimental set up. It consists of three main sections: high pressure chamber, cryogenic heat exchanger, and plumbing for introduction of different substances as ambient media inside the chamber and for routing of the injectants through the injector. The high pressure chamber is

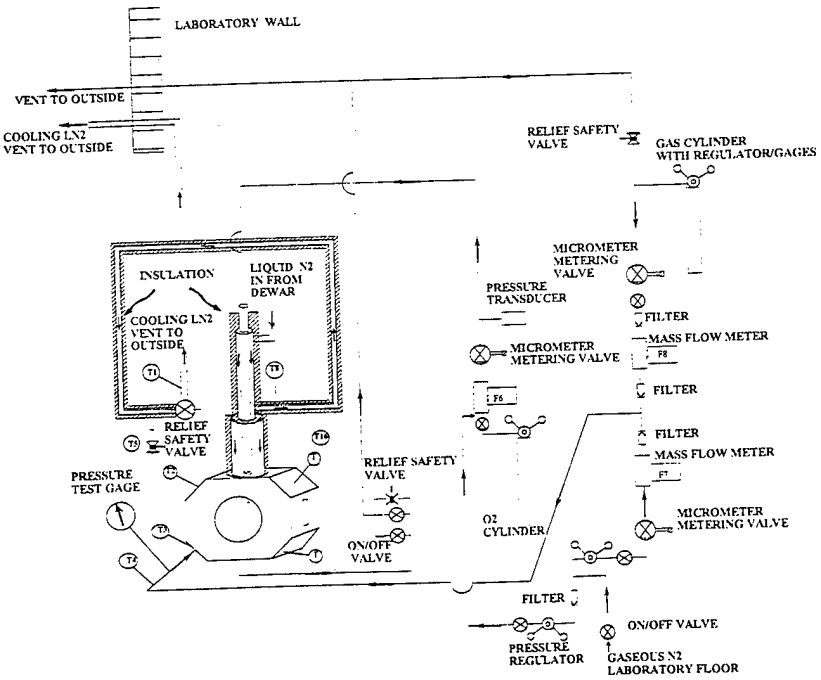


**Figure 1. Schematic diagram of experimental setup for sub- to supercritical jet injection.**

constructed with stainless steel to withstand pressures and temperatures of up to 137 atm (2000 psi) and 473 K, respectively. For optical diagnostics, there are provisions for two facing circular sapphire windows of 133.4 mm (5.25") diameter and two facing UV-grade side-mounted slot-shaped quartz windows of 120.7 mm x 12.7 mm (4.75" x 0.50") for laser in/out of the chamber. The cryogenic cooler uses liquid $N_2$ from a dewar as the cooling medium. The purpose of this cooler is to cool and/or liquify the injectant passing through it. The mass

flow rate of the injectant is regulated and also measured via a mass flowmeter and a precision micrometer valve. For more details refer to *Woodward and Talley [7]*. Back-illuminated arrangement is used for initial visual characterization. A QuadTech Stroboslave with a light diffuser in its front along with a model K2 Infinity long-distance microscope with variable focus and manual iris are used to form images of the injected jets presented in this paper. A TM-745E high resolution (768(H) x 493(V) pixels in 8.8(H)x6.6(V) mm actual sensing area) interlaced CCD camera by PULNix with composite video output is used in free run operating mode. The image is captured by a scientific image grabber LG-3 from Scion Corporation installed in a dedicated Macintosh computer and run by the NIH (National Institute of Health) image acquisition and processing software package for Macintosh. This system provides reliable frame rates of up to 20 frames per second. The injector in this study is a sharp-edged 50 mm long stainless steel tube with 1.59 mm (1/16") diameter and a 254 micron (0.010") inner hole (length-to-diameter ratio of 200). The length is therefore long enough to ensure fully-developed turbulent pipe flow at the exit.

## JET STRUCTURE

Figure 2 shows images of the $N_2$ jet injected into $N_2$ at a fixed supercritical chamber temperature but varying sub- to supercritical pressure. At the lowest subcritical chamber pressure the jet is liquid-like with surface instabilities that grow downstream where it has twisted appearance. At $P_r$ of 0.43 all instabilities are further amplified until at the next higher pressure where many surface ligaments and drops are seen being ejected from the jet. At $P_r$ of 0.83 fine drops are seen surrounding the jet and its spanwise dimension noticeably grows away from the injector exit plane. At $P_r$ of 1.02 the $N_2$ jet enters into a supercritical temperature and near-critical pressure environment. There are drastic changes in details of the interface. There are no detectable drops under this condition with the highest software magnification used to view these high resolution images. There are thread- or finger-like entities emerging from the jet which are not broken up into droplets as before but are seemingly dissolved at a spectrum of distance from the dark core. This, in a sense, forms a mixing layer in which phase transition and/or large local density nonuniformities occur. Any further increase of chamber pressure decreases the length and the thickness of the internal dark core and images progressively resemble injection of a gaseous turbulent gas jet into a gaseous environment. Figure 3 is the magnified images of the mixing layer at three subcritical, transitional, and supercritical chamber pressures. Gradual transition from classical ligament and drop formations at the interface, seen in liquid atomization regime, to where submerged turbulent jet appearance emerges can be observed. These observations are also consistent with images presented by *Mayer et al [6]*. In summary, for $N_2$ into $N_2$ injection at the supercritical ambient temperature tested here, there appears to be two structural transitions. One is when the intact jet with irregularly-looking surface waves and downstream shiny twisted-shaped column turns into a somewhat diverging jet with ligaments and many small droplets. The other is when the latter structure changes into a gas-jet appearance near but below the point where the medium pressure changes from sub- to supercritical conditions (based on the injectant critical pressure). The reason for this manner, particularly for the change into gas-jet behavior, should be sought in progressive reduction of surface tension and heat of vaporization until they both vanish at and above the critical point.

## JET SPREADING ANGLE

Looking at images in Fig. 2, one important geometrical parameter that can be quantitatively evaluated is the jet spreading angle or its growth rate. Therefore, this parameter is measured for all images acquired and results along with those of others are presented in Fig. 4. Of importance in Fig. 4 are the selection of the data sets and the nature of their measurements by other researchers as well as the choices of the axes. Since the jets investigated here exhibit both liquid-jet and gas-jet like appearances, appropriate results for both are shown. For the $N_2$ into $N_2$ case tested in this work, an average curve (not drawn) through the data points in Fig. 4 intersects the *Papamoschou and Roshko's [1]* incompressible variable-density mixing-layer theoretical curve somewhere at the density ratio of 0.09. Departure between the two increases below the critical pressure of $N_2$ where the jet appears liquid-like, going even below the *Dimotakis's[2]* mixing layer equation. Note that the tendency of the data to approach those of liquid sprays generated by a high length-to-diameter ratio nozzle is evident. Data for $O_2$ into $N_2$ shows a steeper drop in angle near but below the critical pressure of oxygen in Fig. 4. To build confidence and also generate gaseous jet data using the identical arrangement, we injected cooled He gas into

the $N_2$ chamber as well as cooled $N_2$ into He environment. Results are shown in Fig. 4 for a range of chamber pressures from 0.77 to 9.19 MPa. Although there is scatter in the data at various chamber pressures, it is interesting that the narrowing of the angle is seen as injection of the cooled $N_2$ into He is considered, consistent with the *Brown and Roshko's [8]* data. The shift to lower density ratios seen in our data is because injectants are cooled in our case. In summary, there is one clear conclusion, that for a range of density ratios in which our images show gas-jet like appearance the experimental data agrees well with the proposed theoretical equation by *Papamoschou and Roshko [1]* and follows the trend of *Dimotakis's* equation. This can be taken as further and quantitative confirmation that at ambient supercritical pressure and temperature conditions (based on the injectant values) the injected jets visually behave like a gas though technically it may be referred to as "fluid". There is marked disagreement between liquid sprays (at comparable length-to-diameter ratio of 85) and our data, see Fig. 4, even though it appears going through initial phases of the atomization process, see Figs. 2. The disagreement is that although the jet studied here shows second wind-induced breakup features, it fails to reach full atomization state as chamber pressure is raised due to decrease in both surface tension and heat of vaporization. Transition into the full atomization region is therefore inhibited. A search for a universal curve to cover all the data in Fig. 4 is a challenging one. To date, no appropriate nondimensionalized parameters are found to collapse all spreading rate information on a single curve. Appropriateness of the surface tension for liquid jets and sprays and its irrelevance for gaseous jets are among the issues to be reconciled.

## SUMMARY AND CONCLUSIONS

Structural transition and growth rate of jets injected into an environment at fixed supercritical temperature but varying sub- to supercritical pressure are analyzed. $N_2$, $O_2$, and He are injected into $N_2$, He, and mixtures of $CO+N_2$ at different proportions. Increasing chamber pressure from a low subcritical value, the fluid in the jet appears to go through classical liquid jet breakup stages up to a second wind-induced breakup regime. In this regime one sees a divergent jet with ligaments and many droplets ejecting from the jet. Penetration into the full atomization regime is inhibited near but before the critical pressure of the injectant because of the combined effects of lowered surface tension and heat of vaporization. At this point the jet assumes a gas-jet like appearance that remains up to the highest pressure tested here. Also, a unique and new plot is formed by converting all other types of spreading rates to the visual growth rate using most relevant works of others on variable density incompressible mixing layers, axisymmetric incompressible and compressible gas jets/mixing layers, and liquid sprays, covering an ambient-to-injectant density ratio range of a 1000. Our measurements clearly follow a theoretical equation proposed by *Papamoschou and Roshko [1]* for an incompressible but variable density turbulent mixing layers. This agreement for spreading angles starts at a pressure near but below the thermodynamic critical value of the injectant substance, quantitatively confirming gas-jet like visual appearance observed in images of the jets for the first time. Therefore, (1) inability of droplet visual detection in the acquired images and their visual impression of a gaseous jet, (2) inhibition of transition into the full atomization zone due to lowered surface tension tested by the available atomization criteria, (3) rapid gasification due to vanishingly small heat of vaporization, and (4) agreement of the jet spreading rate experimental measurements with those of incompressible but variable density gas mixing layers theory, all tend to strengthen the position that at near and above the critical point of the injectant the jet exhibits gas-jet like behavior. Considering this, relevancy of current injection models and some drop vaporization/combustion results under the conditions where gas-jet like behavior is detected should be reexamined.

## REFERENCES


1. Papamoschou, D. and Roshko, A.. "The compressible turbulent shear layer: an experimental study," J. Fluid Mech., vol. 197, 1988, pp. 453-477.
2. Dimotakis, P. E. "Two-dimensional shear-layer entrainment," AIAA Journal, 21, No. 11, 1986, pp. 1791-1796.
3. Lazar R. S. and Faeth, G. M. "Bipropellant droplet combustion in the vicinity of the critical point", Thirteen Symposium (International) on Combustion, The Combustion Institute, P.801, 1971.
4. Newman, J. A. and Brzustowski. "Behavior of a liquid jet near the thermodynamic critical region," AIAA Journal, vol. 9, 1971, no. 8, pp. 1595-1602.

5. Mayer, W., Schik, A., Schweitzer, C., and Schaffler, M. "Injection and mixing processes in high pressure LOX/GH2 rocket combustors," AIAA Paper no. 96-2620, 32nd AIAA/ASME/SAE/ASEE Joint Propulsion Conference & Exhibit, Lake Buena Vista, Florida, 1996.
6. Mayer, W., Ivancic, A., Schik, A., and Hornung, U. "Propellant atomization in LOX/GH2 rocket combustors," AIAA Paper no. 98-3685, 34 the AIAA/ASME/SAE/ASEE Joint Propulsion Conference & Exhibit, Cleveland, Ohio, , July 13-15, 1998.
7. Woodward , R. D. and Talley, D. G. "Raman imaging of transcritical cryogenic propellants," AIAA Paper 96-0468, 34 the AIAA Aerospace Sciences Meeting and Exhibit, Reno, Nevada, January 1996.
8. Brown, G. and Roshko, A. "On density effects and large structure in turbulent mixing layers," J. Fluid Mech., vol. 64, 1974, part 4, pp. 775-816.

Instant images of

# $N_2$ into $N_2$

($P_{critical}$ = 3.39 MPa; $T_c$ = 126.2 K)

($P_{ch}/P_{critical}$= 2.71, 2.41, 2.01, 1.62, 1.22, 1.02, 0.93, 0.82, 0.62, 0.43, 0.23; from upper left to lower right)

(Re= 25,000 to 75,000; injection velocity: 10-15 m/s; Froud: 40,000 to 110,000)

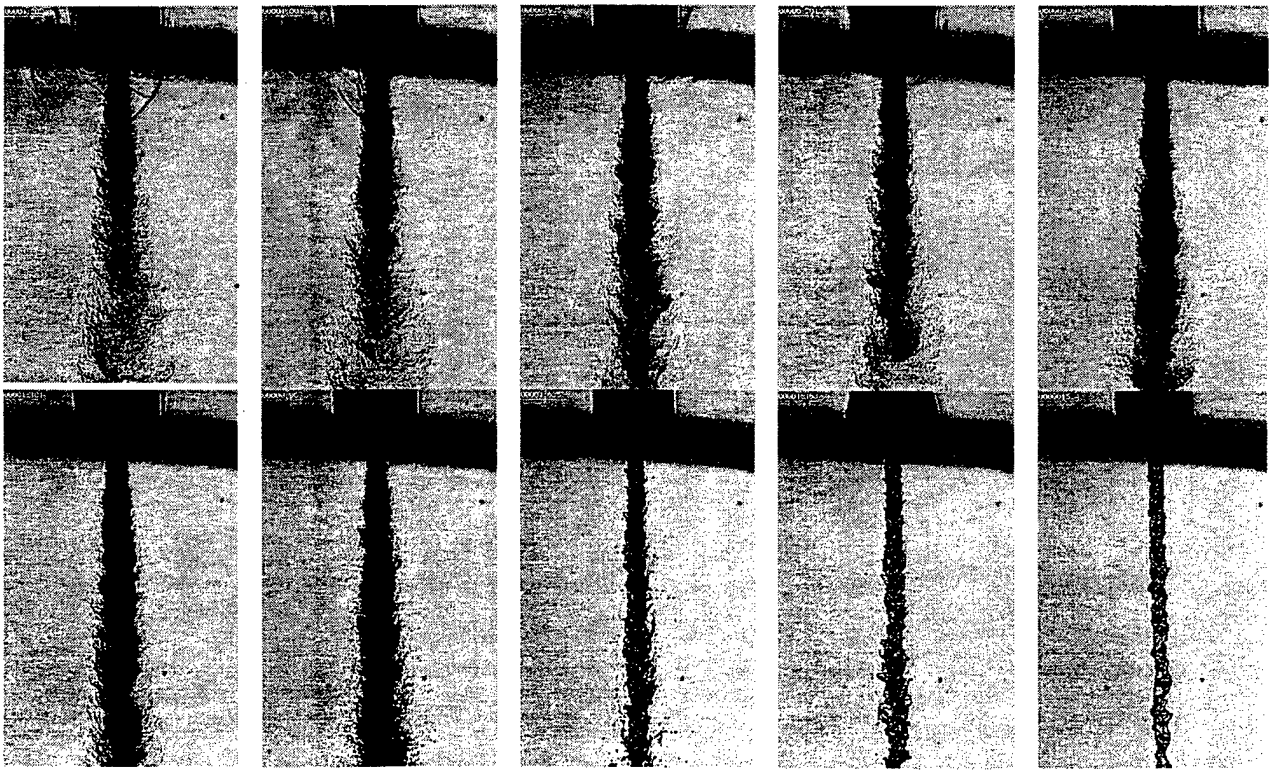

Figure 2. Back-illuminated images of the nitrogen injected into chamber of nitrogen at a fixed supercritical temperature of 300 K but varying sub- to supercritical pressure. Injectant temperature: 99 to 120 K.

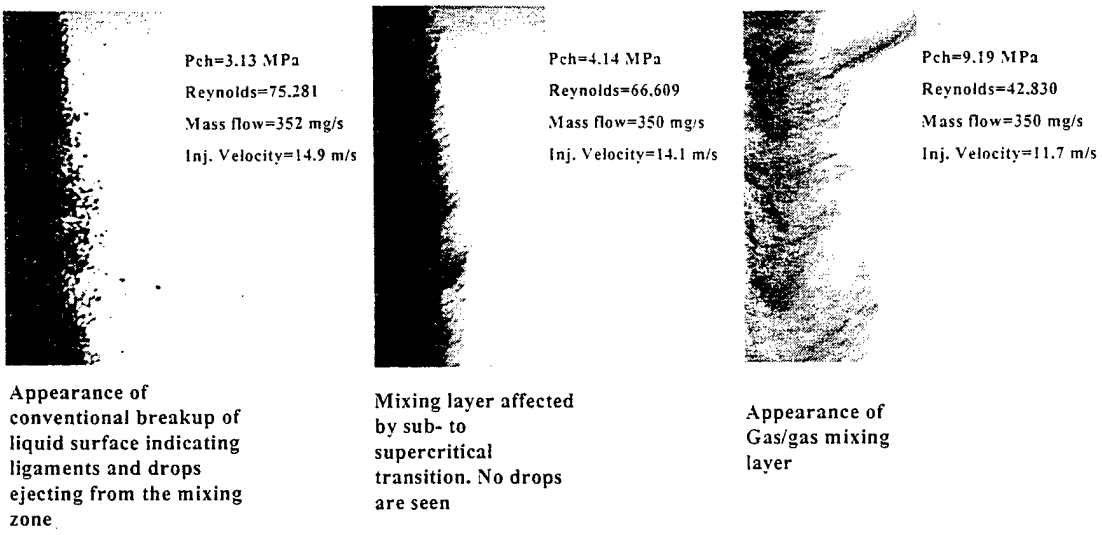


Figure 3. Magnified images of the jet at its outer boundary showing transition to the gas-jet like appearance starting at just below the critical pressure of the injectant. Images are at fixed supercritical chamber temperature of 300 K. Relative pressure: 0.9, 1.22, 2.71 from left to right.

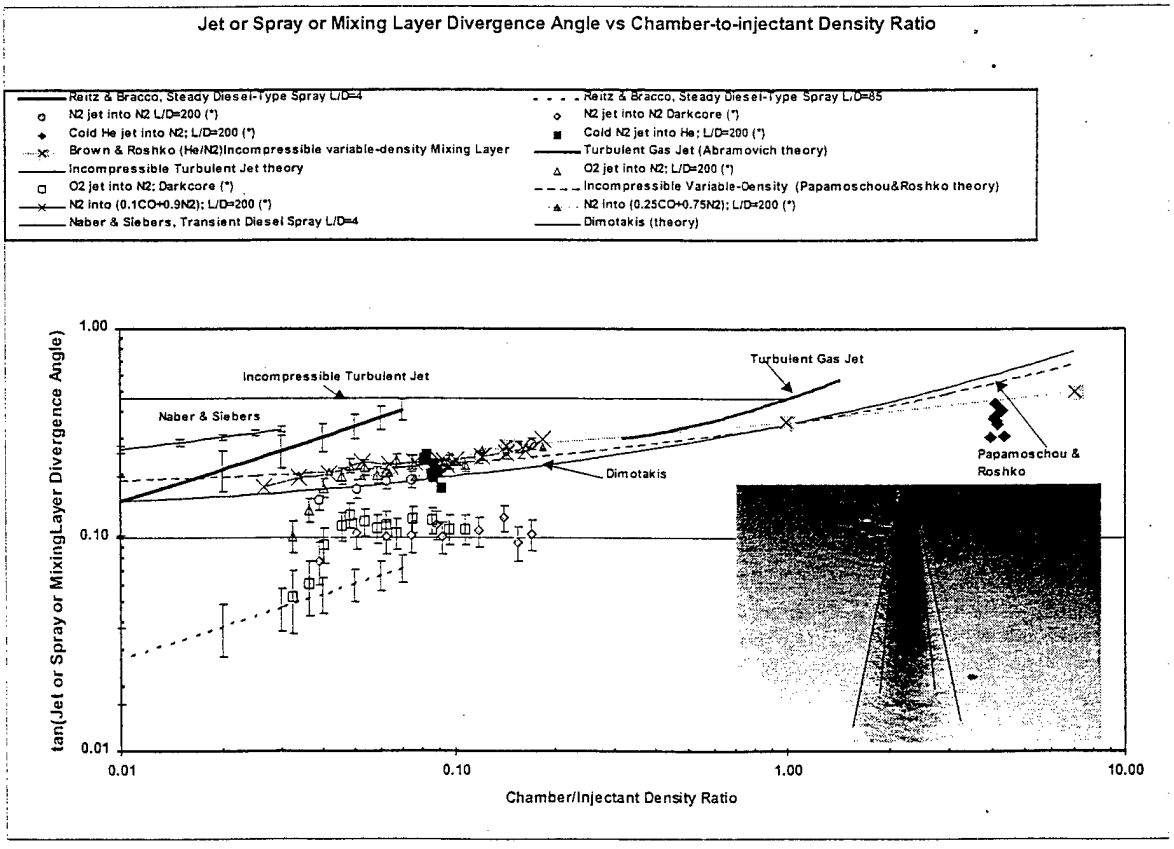


Figure 4. Shows spreading or growth rate as tangent of the visual spreading angle versus the chamber-to-injectant density ratio. (*) refers to data taken at AFRL.